Available online at www.sciencedirect.com
ScienceDirect
Applied Catalysis B: Environmental 80 (2008) 62–71
APPLIED CATALYSIS B: ENVIRONMENTAL
www.elsevier.com/locate/apcatb

Impact of the support oxide and Ba loading on the sulfur resistance and regeneration of Pt/Ba/support catalysts

E.C. Corbos *, X. Courtois, N. Bion, P. Marecot, D. Duprez

Laboratoire de Catalyse en Chimie Organique, UMR 6503 CNRS, Université de Poitiers, 40 avenue du Recteur Pineau, 86022 Poitiers cedex, France

Received 17 July 2007; received in revised form 4 October 2007; accepted 6 October 2007
Available online 13 October 2007

Abstract

The influence of both the support oxide (Al_2O_3, SiO_2, Al_2O_3–5.5 wt% SiO_2 and $Ce_{0.7}Zr_{0.3}O_2$) and the barium loading of Pt/Ba/Support model catalysts on sulfur resistance was investigated by hydrogen temperature programmed reduction (TPR), X-ray diffraction (XRD) and NO_x storage capacity measurements. The sulfation of catalysts under lean conditions in the presence of water and carbon dioxide led to the formation of both surface and bulk sulfates, except for silica supported catalyst on which mainly bulk barium sulfates were formed. Sulfate stability was influenced by the support oxide and the Ba loading. For alumina containing catalysts, both the amount of deposited sulfur and the sulfate stability under hydrogen increase with the Ba loading. Conversely the same sulfates stability was observed for Ce–Zr supported samples, whatever the Ba loading. The thermal treatment of the sulfated catalysts under oxidizing conditions at 800 °C favored the formation of less reducible bulk barium sulfates on all the catalysts. Ceria–zirconia led to a decrease of bulk $BaSO_4$ stability under hydrogen, their reduction temperature being about 100 °C lower than on alumina containing materials. The elimination of sulfates under rich conditions (H_2, CO_2, H_2O, N_2) was more effective on the ceria–zirconia supported sample compared to alumina containing catalysts, even after ageing at 800 °C.

Sulfation of the catalysts induced a loss of NO_x storage capacity depending on catalyst composition. All the catalysts recovered their initial NO_x storage capacity after regeneration at 550 °C, even with an improvement in the case of the ceria–zirconia supported material. The ageing at 800 °C of sulfated catalysts before regeneration did not lower the performance of the Pt/10Ba/CeZr catalyst, contrary to the alumina containing samples.

Keywords: NO_x storage; Barium sulfate; Ceria–zirconia; Alumina; Silica; Sulfur elimination; Regeneration

1. Introduction

In order to improve air quality, more and more stringent regulations are imposed to automotive manufacturers, especially for diesel and direct injection gasoline engines. These engines, operating under an excess of oxygen (lean conditions), have a potential to improve fuel efficiency and so to reduce CO_2 emissions. However, excess of oxygen prevents conventional three-way catalysts from working effectively to reduce NO_x. A promising solution to overcome this issue was introduced in the mid-1990s by Toyota with the concept of NO_x storage-reduction (NSR) [1]. This concept is based on the NO_x storage by forming chemical compounds with a storage material under lean conditions followed by a short incursion in rich atmosphere (excess of hydrocarbons) where the stored NO_x are released and reduced into N_2.

Typically, NSR systems contain three major components: a basic storage material (alkaline or alkaline earth oxides, e.g. BaO), a component for NO_x oxidation/reduction (precious metals, e.g. Pt) deposited on a high surface support oxide (e.g. Al_2O_3) [2]. Nevertheless, the NSR systems are sensitive to sulfur (present in oils and gasoline) and temperature. It is known that, under lean conditions, SO_2 coming from sulfur oxidation leads to the deactivation of NSR catalysts, due to the formation of stable sulfates which block storage sites [2–25]. The poisoning is reversible, and sulfates can be partly eliminated in rich conditions at high temperatures (600–750 °C) [8–12]. However, successive regenerations result in thermal deactivation of the catalyst [2]. The effect of sulfur was widely studied on Pt/Ba/Al catalysts [2–15]. The well dispersed

* Corresponding author. Tel.: +33 549453994; fax: +33 549453741.
E-mail address: elena.cristina.corbos@etu.univ-poitiers.fr (E.C. Corbos).

0926-3373/$ – see front matter
doi:10.1016/j.apcatb.2007.10.009

barium sulfates located in Pt proximity are reducible at low temperatures whereas bulk-like species are reducible at relatively higher temperatures [5,9–12]. The regeneration of the storage component also depends on time [9] and on the nature of the reductant [12,13]. Hydrogen is more effective than carbon monoxide which is itself more effective than hydrocarbons [12,13]. Under rich conditions, sulfides are formed on the platinum particles, thus blocking the metal surface and hindering the further reduction function of the metal [15,16]. Moreover, under hydrogen, a part of sulfur is still present on the catalyst as barium sulfides, which are re-oxidized into sulfates under lean conditions leading to the poisoning of some storage sites. Nevertheless, it has been shown that sulfide formation is avoided when CO_2 and H_2O are present in the regeneration mixture [5,10].

Different strategies have been applied in order to improve sulfur resistance. One was to keep barium as storage material and to modify its properties by adding different compounds in order to decrease the desorption temperature of sulfates or prevent their formation: Fe [17], Mg [18], Li [4]. Matsumoto et al. [4] also investigated the role of the support oxide on sulfur resistance and showed that the stronger is the acidity of the support oxide the less is the amount of deposited sulfur. They concluded that an optimum of the acidity needs to be found in order to improve sulfur resistance and proposed an alumina–titania containing catalyst, with improved sulfur resistance. The mixing of a $Pt/Ba/Al_2O_3$ catalyst with $Mn/Ba/Al_2O_3$ led to the formation of stable Mn sulfates over the latter and prevented the $Pt/Ba/Al_2O_3$ catalyst from significant poisoning, thus maintaining a high NO_x storage in the presence of SO_2 [19]. Hodjati et al. [20] showed that a $BaSnO_3$ perovskite type material presents a good NO_x adsorption capacity in the presence of SO_2 at low temperature (200 °C).

Other researchers attempted to enhance sulfur resistance of NSR catalysts by changing the storage material. Huang et al. [21] improved sulfur resistance of the catalyst by substituting barium oxide for TiO_2. They concluded that although the barium containing material had a better NO_x storage capacity in the absence of SO_x, a Pt-Rh-Al_2O_3-TiO_2 catalyst was more suitable on account of its superior sulfur resistance. They explained these results by a lower decomposition temperature of sulfates on TiO_2. Takahashi et al. [22] studied potassium containing catalysts and pointed out that an acidic mixed oxide (70 wt% ZrO_2–30 wt% TiO_2) was the best support against sulfur poisoning. Yamamoto et al. [23] used a $Pt/LiO_2/TiO_2$ catalyst as NSR sorbent with high sulfur resistance. Centi et al. [24] proposed a PtCu catalyst deposited on a Mg–Al support oxide obtained from a hydrotalcite type precursor and Clacens et al. [25] developed a non noble thioresistant NO_x trap by blending Cu/ZrO_2 with a potassium/alumina material as active NO_x storage catalysts with improved sulfur resistance, Cu being not able to oxidize SO_2 into SO_3.

We have reported recently [26] that the support oxide (Al_2O_3, SiO_2, Al_2O_3–5.5SiO_2 and $Ce_{0.7}Zr_{0.3}O_2$) and Ba loading influence both the catalyst basicity and Pt–Ba proximity, and thus catalyst performances in the presence of water and CO_2. In this paper, we further focus our attention on the critical question of catalyst deactivation by SO_2 for previously studied samples. The effect of the thermal ageing under oxidizing conditions of sulfated catalysts was also investigated together with the regeneration of sulfated catalysts under hydrogen in the presence of CO_2 and H_2O. These effects were investigated on the rapid NO_x storage of catalysts under realistic conditions, i.e. in the presence of CO_2 and H_2O at 300 °C.

2. Experimental

2.1. Catalyst preparation, sulfation and regeneration

Four oxides were studied: (γ)-Al_2O_3 (Al), SiO_2 (Si), Al_2O_3–5.5% SiO_2 (Al5.5Si) and $Ce_{0.7}Zr_{0.3}O_2$ (CeZr) as barium support for NO_x traps. The Pt/xBa/support (where x is the loading in wt% of BaO and support represents the support oxide) catalysts were prepared using the following method. The support was first calcined at 500 °C for 4 h under air and then impregnated with a barium nitrate solution, in order to obtain a 5, 10, 15, 20 or 30 wt% BaO content. After drying at 120 °C for 12 h, the barium containing support was calcined at 700 °C (heating rate 5 °C/min) under air for 4 h. The resulting powder was then impregnated with a dinitro-diamino platinum solution in order to obtain a 1 wt% Pt catalyst. After drying, the catalyst was calcined at 450 °C under air for 2 h and then activated at 700 °C for 4 h under a mixture containing 10% O_2, 10% H_2O, and N_2. Pt/support catalysts were prepared following the same protocol by adding platinum to the unmodified support.

In the sulfation process, the catalyst sample was exposed to a 100 ppm SO_2, 10% CO_2, 10% O_2, 10% H_2O and N_2 mixture at 300 °C for 5 h. After flushing at 300 °C under 10% CO_2, 10% O_2, 10% H_2O and N_2 mixture for 15 min, the catalyst was cooled down to room temperature under the same mixture. Water was removed from the flow at 100 °C. The amount of SO_2 introduced during the sulfation treatment corresponds to a 2.0 wt% S content if all the sulfur is stored on the catalyst. The sulfated catalysts are denoted Pt/xBa/support + S. Also, the effect of a thermal treatment under oxidizing conditions was studied. Samples of the sulfated catalysts were aged at 600 °C and 800 °C for 30 min under a mixture containing: 10% O_2, 10% CO_2, 10% H_2O and N_2. The catalysts are then denoted Pt/xBa/support + S Ty (y: temperature of the final thermal treatment).

The regeneration of the sulfated catalysts was done with a rich mixture containing 2.5% H_2, 10% CO_2, 10% H_2O and N_2. The catalysts were heated under this mixture from room temperature (except for H_2O, 100 °C) up to the regeneration temperature (500 °C or 550 °C, heating rate: 10 °C min^{-1}) and maintained at this temperature for 30 min before cooling under N_2.

2.2. NO_x storage capacity measurements

The NO_x storage capacities of the catalysts were measured at 300 °C. Before the NO_x storage capacity measurements, the catalyst sample (60 mg, particles diameter 0.1–0.25 mm) was pretreated at 300 °C for 30 min under a 10% O_2, 10% H_2O,

10% CO_2 and N_2 mixture (total flow rate: 10 L h^{-1}). The sample was then submitted to a 350 ppm NO, 10% O_2, 10% H_2O, 10% CO_2 and N_2 mixture (total flow rate: 10 L h^{-1}). The gas flow was introduced using mass-flow controllers, except for H_2O vapors which were introduced using a saturator thermostated at 46 °C. Both NO and NO_x concentrations ($NO + NO_2$) were followed by chemiluminescence with a COSMA Topaze 2020 apparatus. H_2O was removed prior to NO_x analysis with a membrane dryer. The NO_x storage capacity was calculated by the integration of the recorded profile for the first 100s and platinum oxidation activity was estimated at saturation (usually about 900s) as the NO_2/NO_x ratio (%). Under the conditions used in NO_x storage measurements (60 mg, 10 L h^{-1}, 350 ppm NO) a maximum of 67 μmol NO_x per gram of catalyst can be stored. This corresponds to the complete trapping of NO_x injected on the catalyst in 100s.

2.3. Catalyst characterizations

The *in-situ* XRD measurements at different temperatures were carried out in an Anton PAAR HTK16 high-temperature stainless chamber linked to a Siemens D8 (Bragg–Brentano θ–θ) powder diffractometer. The powders were supported on a Kanthal foil. The powders were heated under air to the desired temperature with a heating rate of 10 °C min^{-1}. Diffractogramms were recorded from $2\theta = 10–70°$, with an increment of 0.02° 2θ, dwell time 2 s at 25 °C and after annealing the catalysts for 0.5 h at 600 °C and 800 °C. The crystalline phases were identified by comparison with the ICDD database files

The BET surface areas were deduced from N_2 adsorption at −196 °C carried out with a Tristar 3000 Micromeritics apparatus. Prior to the measurement, the samples were pretreated at 350 °C under vacuum for 12 h in order to eliminate the adsorbed species. The BET surface areas of the support oxides were 144 $m^2 g^{-1}$, 147 $m^2 g^{-1}$, 317 $m^2 g^{-1}$, and 80 $m^2 g^{-1}$ for Al_2O_3, SiO_2, Al_2O_3–5.5 wt% Si and $Ce_{0.7}Zr_{0.3}O_2$, respectively. The BET surface areas of the catalysts are listed in Table 1.

2.4. Temperature programmed reduction (TPR)

Prior to the TPR, the catalyst (65 mg) was first pretreated *in situ* under oxygen at 300 °C for 30 min and cooled to room temperature. After flushing under argon for 45 min, the reduction was carried out from room temperature up to 800 °C under a 1% H_2/Ar mixture, using a 5 °C min^{-1} heating rate. The sample was maintained at 800 °C for 30 min before cooling under argon. Hydrogen consumption was followed by thermal conductivity.

Table 1
BET surface areas of the Pt/*x*Ba/support catalysts

Support	Al		Si		Al5.5Si			CeZr		
BaO (wt%)	10	20	10	20	10	20	30	5	10	20
BET ($m^2 g^{-1}$)	126	74	106	78	319	200	160	56	43	27

3. Results and discussion

3.1. Influence of the support oxide on sulfate stability under hydrogen

It is well known that the presence of sulfur species in the exhaust gas leads to the formation of sulfates deactivating thus the NSR catalysts [2–15]. To further investigate the way the support oxide may influence sulfates formation and their stability, the different materials were sulfated under oxidizing conditions at 300 °C in order to obtain a sulfur content of 2 wt% if all sulfur was deposited on the catalyst. To obtain information about the stability of sulfur species and the amount of deposited sulfur, the sulfated catalysts were characterized by TPR under hydrogen.

Fig. 1 shows the TPR profiles of the different sulfated catalysts. The hydrogen consumptions and the corresponding amounts of deposited sulfur are listed in Table 2.

Fig. 1 and Table 2 show that both sulfate stability under hydrogen and the amount of deposited sulfur are influenced by the support oxide and the Ba loading. In order to determine the effect of sulfating at 300 °C on the formation of aluminum sulfates, a Pt/Al catalyst was sulfated at 300 °C and then characterized by TPR. The reduction profile of the sulfated Pt/Al catalyst shows a hydrogen consumption between 350 °C and 700 °C (Fig. 1a). The peak near 450 °C corresponds to the reduction of surface aluminum sulfates located in the platinum proximity while hydrogen consumption at higher temperatures can be attributed to the reduction of aluminum sulfates more and more distant from the metal function. The TPR profile of the sulfated Pt/20Ba/Al catalyst shows the presence of three main peaks (Fig. 1a). When comparing the TPR profile of the sulfated Pt/Al catalyst with that of the Pt/20Ba/Al catalyst (Fig. 1a) it can be observed that the latter presents a peak near 450–500 °C more intense than the Pt/Al catalyst. These results indicate that in this temperature range the reduction of aluminum sulfates takes place simultaneously with the reduction of some well dispersed barium sulfates, located in platinum proximity. The two other peaks observed around 650 °C and 750 °C for the Pt/20Ba/Al catalyst are ascribed to the reduction of surface and bulk barium sulfates, respectively. It is known in the literature [5,11], that barium sulfates reduction depends on their size and location towards platinum particles, small surface sulfates located in the platinum proximity being easily reducible. On the other hand, the reduction of large barium sulfates (bulk like species >10 nm) is mostly relied on gas–solid phase reaction between sulfates and H_2 [11]. The decrease of the Ba loading for the Pt/Ba/Al catalysts induces mainly a decrease of the H_2 consumption for the reduction of bulk barium sulfates (Fig. 1a). Nevertheless, decreasing the Ba loading tends to shift the surface sulfate reduction temperatures. This result may be explained by previous characterizations of these samples [26], showing different Pt–Ba proximity linked to different Pt and Ba dispersions.

Assuming a H_2/SO_4^{2-} ratio of 4 for the sulfate reduction ($X\text{-}SO_4 + 4H_2 \rightarrow X\text{-}S + 4H_2O$ and/or $X\text{-}SO_4 + 4H_2 \rightarrow X\text{-}$

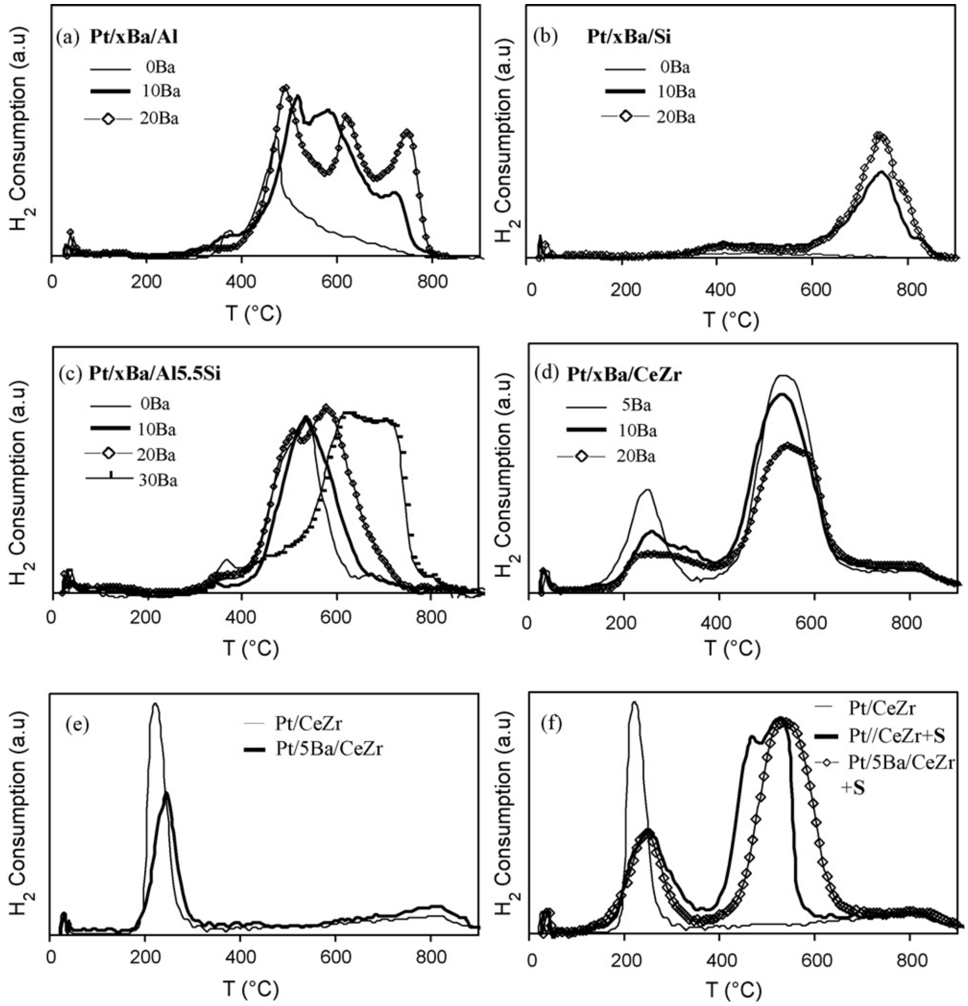

Fig. 1. TPR profiles of sulfated catalysts. Sulfation was carried out at 300 °C under oxidizing conditions.

$O + H_2S + 3H_2O$), a total sulfur content of 1.9 wt% on the Pt/20Ba/Al catalyst was deduced from hydrogen consumption (Table 2). This value is very close to the amount of sulfur injected in the gas flow during the sulfation treatment (2 wt%). The lower amounts of sulfur deposited on the Pt/10Ba/Al (1.6 wt% S) and Pt/Al (0.7 wt% S) catalysts confirm that the barium component is more active than alumina for sulfate formation.

No significant sulfur deposition was observed after the sulfation treatment of the Pt/SiO_2 catalyst (Fig. 1b) in agreement with previous works reported in the literature [27]. The addition of the Ba component to the material led to the formation of barium sulfates with a main reduction peak between 600 °C and 800 °C, whatever the barium loading is, as indicated by the TPR profiles (Fig. 1b). This peak, with a maximum near 750 °C was attributed to the reduction of bulk barium sulfates. The small hydrogen consumption observed between 350 °C and 600 °C may correspond to the reduction of very few surface barium sulfates. This result is in agreement with the very low NO_x storage capacities measured on silica supported catalysts and reported in a previous work [26]. The low amounts of deposited sulfur, 0.7 wt% and 0.9 wt% for Pt/10Ba/Si and Pt/20Ba/Si, respectively, are mainly explained by both the absence of sulfate deposition on the SiO_2 support and the lower rate for bulk barium sulfation in comparison with surface species [15].

The alumina–silica supported catalysts present a similar behavior with alumina supported materials. Sulfate stability and the amount of sulfur increase with the Ba loading (Fig. 1c and Table 2). The TPR profile of the sulfated Pt/Al5.5Si catalyst

Table 2
H_2 consumptions during TPR of sulfated catalysts and sulfur contents (wt%)

Support	Al			Si			Al5.5Si				CeZr			
BaO (wt%)	0	10	20	0	10	20	0	10	20	30	0	5	10	20
H_2 (mmol g^{-1})	0.87	1.95	2.40	0.05	0.86	1.06	1.41	1.53	2.27	2.45	1.58	1.72	1.61	1.14
S (wt%)	0.70	1.56	1.92	∼0	0.67	0.85	1.13	1.22	1.82	1.96	1.26	1.38	1.29	0.91

indicates that the reduction of aluminum sulfates takes place between 350 °C and 700 °C, as previously observed for the sulfated Pt/Al catalyst. However, the reduction peak is more intense than for the Pt/Al sample. the higher surface area of the alumina–silica support compared with the alumina support (319 $m^2 g^{-1}$ versus 144 $m^2 g^{-1}$, respectively) allows one to explain this result since mainly surface sulfates are formed on alumina [3,6]. The Pt/10Ba/Al5.5Si catalyst shows only one reduction peak near 500 °C, slightly larger than that of the Pt/Al5.5Si catalyst (1.2 wt% S versus 1.1 wt% S). This peak was attributed, as previously for alumina supported materials, to the reduction of both aluminum sulfates and well dispersed barium sulfates located in platinum proximity. Increasing the Ba loading to 20 wt% BaO led to the appearance of a second peak near 600 °C which can be attributed to the reduction of more crystallized surface barium sulfates. Finally, the increase of the Ba content to 30 wt% BaO favored the formation of less reducible barium sulfates indicated by the drop of the hydrogen consumption between 400 °C and 600 °C, and the apparition of a broad peak in the 600–800 °C temperature range. This evolution is linked to the formation of bulk barium sulfates to the detriment of well dispersed surface barium sulfates. These results are in agreement with the XRD measurements on the Pt/Ba/Al5.5Si materials, reported in a previous work [26], pointing out that the $BaCO_3$ phase was detected only on the Pt/30Ba/Al5.5Si catalyst. Under a SO_2 containing mixture bulk carbonates on this sample are progressively replaced by bulk barium sulfates.

The TPR profiles of the sulfated ceria–zirconia containing samples are depicted in Fig. 1d. For comparison, the reduction curve of the fresh Pt/CeZr catalyst is also reported (Fig. 1e). This curve shows a main reduction peak near 220 °C attributed to the reduction of Ce^{4+} to Ce^{3+} promoted by platinum [28,29]. The hydrogen consumption corresponds approximately to the reduction of three layers of cerium (the surface and two bulk layers). The small wave of hydrogen consumption at higher temperatures (400–800 °C) is related to the reduction of deeper bulk cerium atoms (Fig. 1e). Fig. 1e shows that the addition of BaO to ceria–zirconia support led to a slight shift of the main reduction peak of ceria to higher temperatures. Sulfation of the Pt/CeZr catalyst led to both a broadening of the low temperature peak with a shift of the maximum to higher temperatures (250 °C versus 220 °C) and the appearance of a large peak between 400 °C and 600 °C (Fig. 1f). The latter corresponds to the reduction of surface and bulk sulfates formed on ceria–zirconia support [3,30]. The addition of barium to ceria–zirconia induced a shift of the reduction of sulfates to higher temperature (Fig. 1f). Nevertheless, all the sulfates are reduced before 650 °C regardless of the Ba loading (Fig. 1d). Surprisingly, the amount of deposited sulfur for ceria–zirconia catalysts decreases as the Ba loading increases (Table 2): 1.4 wt% for Pt/5Ba/CeZr, 1.3 wt% for the Pt/10Ba/CeZr and 0.9 wt% S for the Pt/20Ba/CeZr catalyst, with no significant changes in sulfate stability. The decrease of the amount of sulfur might be due to both the lower BET surface area of the materials with higher Ba loadings (Table 1) and the limitation of SO_x species diffusion in the bulk at 300 °C due to higher barium particles (19 nm for Pt/5Ba/CeZr versus 51 nm for Pt/10Ba/CeZr [26]).

3.2. NO_x storage capacity of sulfated catalysts

The NO_x storage capacities of sulfated Pt/Ba/Al, Pt/Ba/Al5.5Si and Pt/Ba/CeZr catalysts were measured at 300 °C, in order to appreciate the impact of sulfur on the NO_x trapping properties. Pt/Ba/Si catalysts are not discussed in this part since their NO_x storage capacities are already very low before sulfur poisoning [26]. In real engines water and CO_2 are always presents, therefore the NO_x storage measurements were carried out in a mixture containing 10% O_2, 10% CO_2, 10% H_2O, 350 ppm NO and N_2. The results are reported in Fig. 2. For comparison the NO_x storage capacities of the fresh (non-sulfated) catalysts are also reported.

As expected, sulfation leads to a significant decrease of the NO_x storage capacity that ranges between 50 and 70%, depending on catalyst composition. The Pt/20Ba/Al5.5Si catalyst shows the higher NO_x storage capacity (11.1 µmol g^{-1}) after the sulfation treatment. This catalyst, together with the ceria–zirconia supported samples present the lower sensitivity to sulfur with near 50% of loss of their initial NO_x storage capacities. On the contrary, the alumina supported samples present the higher sulfur sensitivity, with approximately 70% of loss of the NO_x storage capacity after sulfation.

In previous work, it was reported that NO_x trapping ability decreased with the increase of the amount of SO_2 injected on the catalyst [31]. In our case, there is no direct correlation between the NO_x storage capacity of the catalysts after sulfation and the amount of deposited sulfur (Fig. 2 and Table 2). The difference may come from the fact that in their study, Engstrom et al. [31] added the SO_2 in the course of the NO_x storage measurement whereas we carried out the sulfation treatment before the NO_x storage.

Fig. 2 shows that the catalysts did not entirely lose their NO_x storage capacity, even if all the sulfur injected during sulfation was not deposited that is to say some sulfur was not able to adsorb on the catalyst. This result may be partially explained by the fact that a part of less stable surface sulfites and/or sulfates desorbs during the flushing carried out for 15 min after sulfation at 300 °C under the H_2O, O_2 and CO_2 mixture. Indeed, Abdulhamid et al. [6] showed by FTIR measurements that the

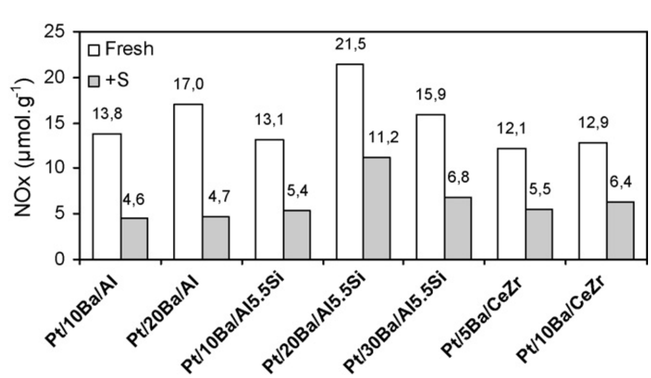

Fig. 2. NO_x storage capacities at 300 °C of fresh and sulfated catalysts.

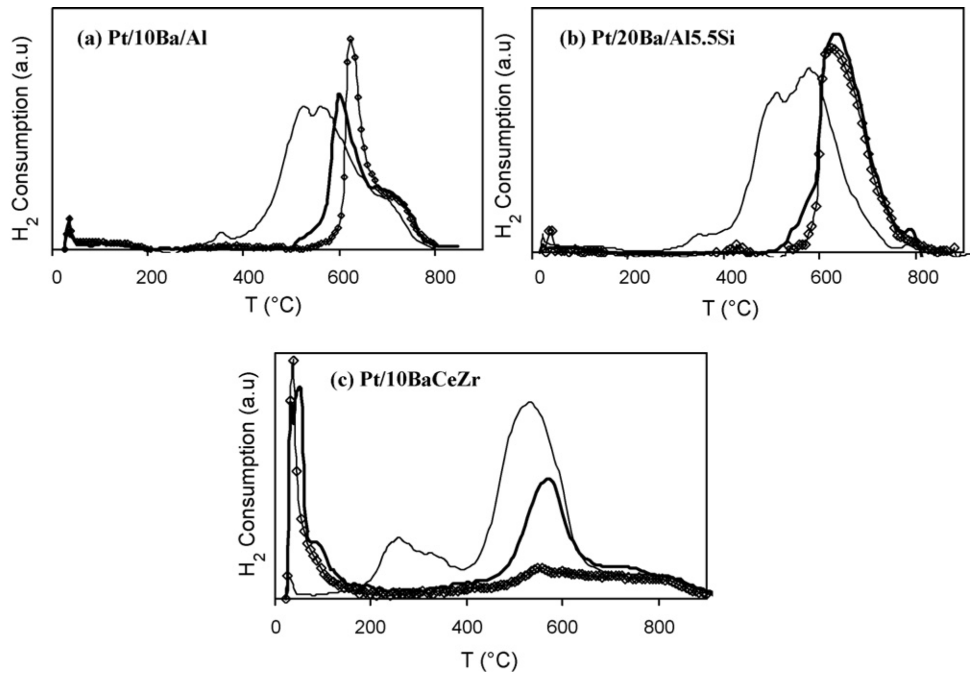

Fig. 3. TPR profiles of (a) Pt/10Ba/Al, (b) Pt/20Ba/Al5.5Si and (c) Pt/10Ba/CeZr. (—) Sulfated; (▬) sulfated and regenerated at 500 °C; (◇) sulfated and regenerated at 550 °C. The regeneration was carried out under a mixture containing H_2, CO_2, H_2O and N_2.

presence of water under lean conditions would lead to a decrease in the formation of surface barium sulfates. A direct consequence is a more or less deep ‘‘regeneration’’ of some surface sites which are able to retain NO_x. Moreover, the formation of sulfates on the catalyst may also lead to a decrease of the material basicity and thus modify the NO_x/CO_2 adsorption competition in favor of NO_x [26].

3.3. Regeneration under a H_2, CO_2 and H_2O mixture

The regeneration of sulfated catalysts was investigated at 500 °C and 550 °C. In previous studies [5,10], it was shown that the regeneration of a sulfated Pt/20Ba/Al catalyst under a mixture containing H_2, CO_2 and H_2O at 650 °C led to a total recovery of the NO_x storage capacity, even if some sulfur species are still present on the catalyst. In order to determine the way the support may influence the regeneration efficiency, the sulfated Pt/10Ba/Al, Pt/20Ba/Al5.5Si and Pt/10Ba/CeZr catalysts were characterized by TPR and NO_x storage capacity measurements after a regeneration treatment at 500 °C or 550 °C for 0.5 h under a mixture containing CO_2, H_2O, H_2 and N_2.

Fig. 3 depicts the TPR profiles of the regenerated catalysts. The TPR profiles of the sulfated catalysts are also reported for comparison. The amounts of remaining sulfur after the regeneration treatments are presented in Table 3. After regeneration at 550 °C, around 40% of the deposited sulfur are eliminated for the sulfated Pt/20Ba/Al5.5Si, around 50% for the sulfated Pt/10Ba/Al and more than 85% for the Pt/10Ba/CeZr (Table 3). Moreover, a stabilization of the remaining sulfates was observed in the case of the alumina and alumina–silica based materials as indicated by the shift of the reduction peak to higher temperatures (Fig. 3a and b). These results show that the regeneration treatment at 550 °C led not only to sulfates elimination but also to a stabilization of some sulfur species previously formed at 300 °C during the sulfation.

For the Pt/10Ba/CeZr catalyst, the regeneration treatment led to a shift of the reduction temperature of ceria oxide to lower temperature (Fig. 3c). Ceria reduction promoted by platinum, starts from ambient temperature and finishes near

Table 3

H_2 consumption and amount of sulfur for sulfated catalysts (S), sulfated and aged at 600 °C or 800 °C catalysts (S T600 and S T800), sulfated and regenerated at 500 °C and 550 °C under H_2, CO_2, H_2O (S R500, S R550) and sulfated, aged and regenerated at 550 °C (S T600 R550 and S T800 R550)

Catalyst		Treatment						
		+S	+S R500	+S R550	+S T600	+S T800	+S T600 R550	+S T800 R550
H_2 (mmol g^{-1})	Pt/10Ba/Al	1.95	0.95	0.86	1.82	1.78	1.50	1.71
	Pt/20Ba/Al5.5Si	2.27	1.52	1.34	2.20	2.24	1.38	1.95
	Pt/10Ba/CeZr	1.61	0.81	0.20	1.60	1.45	0.58	0.70
S (wt%)	Pt/10Ba/Al	1.56	0.76	0.69	1.45	1.42	1.20	1.37
	Pt/20Ba/Al5.5Si	1.82	1.22	1.07	1.76	1.79	1.10	1.56
	Pt/10Ba/CeZr	1.29	0.64	0.16	1.28	1.16	0.46	0.56

200 °C for the regenerated sample while it presents a maximum near 250 °C for the sulfated catalyst. This may be linked to the reduction of platinum particles and/or to a structural re-organization of ceria–zirconia [28] during the regeneration treatment under H_2, CO_2 and H_2O.

Interestingly, if the regeneration temperature is decreased from 550 °C to 500 °C, the amount of eliminated sulfur (Table 3) does not decrease significantly for the Pt/10Ba/Al catalyst (about 0.7 wt% S is present after regeneration at 550 °C and 0.8 wt% S for 500 °C). Furthermore, the regeneration at 500 °C does not lead to sulfate stabilization as in the case of the catalyst regenerated at 550 °C, indicating that sulfate stabilization on such material get start at a temperature above 500 °C. The sulfated Pt/20Ba/Al5.5Si catalyst does not present the same behavior than the Pt/10Ba/Al sample, since a stabilization of sulfated species was observed even after regeneration at 500 °C. Furthermore, the amount of eliminated sulfur increases with the regeneration temperature: near 30% and 40% of S were eliminated after regeneration at 500 °C and 550 °C, respectively. The same behavior regarding sulfur elimination was observed for the Pt/10Ba/CeZr catalyst but the regeneration treatment takes place without any sulfate stabilization: 50% of deposited sulfur were eliminated after regeneration at 500 °C compared to ~90% after regeneration at 550 °C. These results show the interest for the introduction of ceria–zirconia oxides in the NSR formulations, on account of the lower barium sulfates stability under reducing atmosphere compared to alumina containing materials.

3.4. Thermal ageing of sulfated catalysts

As in real engines, the temperature of the exhaust gas may reach temperatures as high as 700–800 °C or even more, we wanted to investigate the effect of thermal ageing of sulfated catalysts under oxidizing conditions on the efficiency of the subsequent regeneration treatment. Sulfated catalysts were aged at 600 °C and 800 °C under oxidizing conditions, and then regenerated at 550 °C. Fig. 4 presents the TPR profiles of sulfated and aged catalysts. For comparison the TPR profiles of sulfated catalysts are also reported. The corresponding hydrogen consumptions and the quantities of stored sulfur are reported in Table 3.

For alumina containing catalysts (Pt/10Ba/Al and Pt/20Ba/Al5.5Si), the oxidizing treatment at 600 °C led to the elimination of aluminum sulfates and to the stabilization of barium sulfates with no significant sulfur elimination (Fig. 4a and b, Table 3), in agreement with previous works [5]. Increasing the temperature to 800 °C led to an increase of the hydrogen consumption attributed to the reduction of bulk barium sulfates (peak at 750 °C). The same behavior was observed for the Pt/10Ba/CeZr catalyst (Fig. 4c), but to a lower extent since after annealing at 800 °C sulfate reduction was mainly completed near 700 °C instead of 800 °C on alumina containing materials. In order to check if bulk barium sulfates are formed during the ageing treatments at 600 °C and 800 °C, the ageing of sulfated Pt/10Ba/Al and Pt/10Ba/CeZr catalysts was followed by *in situ* XRD. The spectra were recorded *in situ* after annealing the catalysts at 600 °C and 800 °C under air for 0.5 h. On the sulfated catalysts, no peak corresponding to crystallized barium sulfates was observed at room temperature regardless of the catalyst (Fig. 5). This result does not exclude their formation, but the amount would be very small and the XRD peak is not detectable. As the TPR profile of the sulfated Pt/10Ba/Al catalyst shows (Fig. 1a), the hydrogen consumption near 750 °C attributed to the reduction of bulk barium sulfates is indeed very small. The XRD spectra of the sulfated catalysts

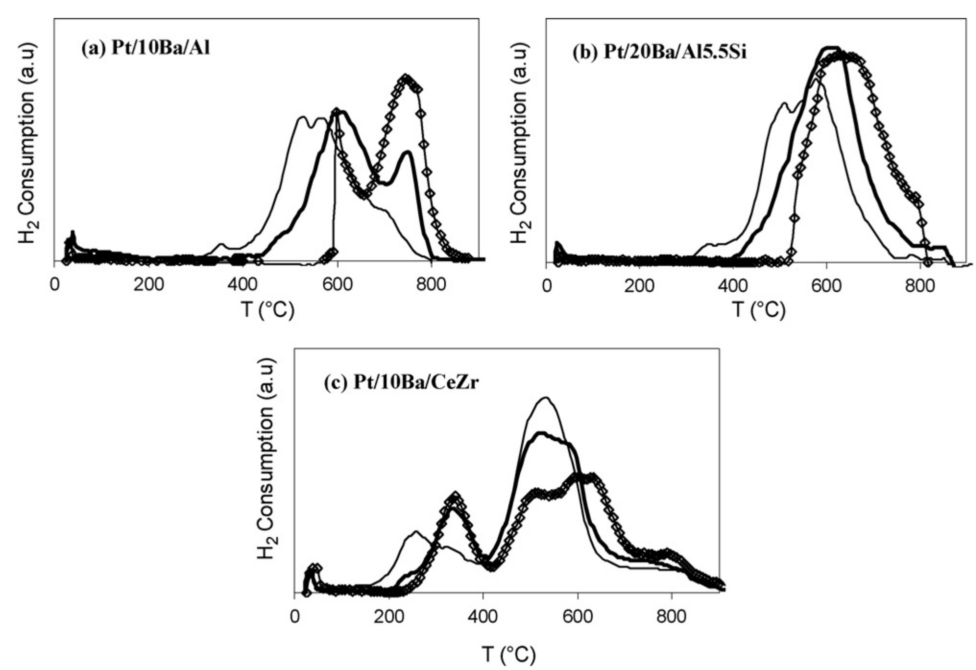

Fig. 4. TPR profiles of (a) Pt/10Ba/Al, (b) Pt/20Ba/Al5.5Si and (c) Pt/10Ba/CeZr. (—) sulfated; (▬) sulfated and aged at 600 °C; (◇) 800 °C sulfated and aged at 800 °C. The ageing was carried out under a mixture containing O_2, H_2O, CO_2 and N_2.

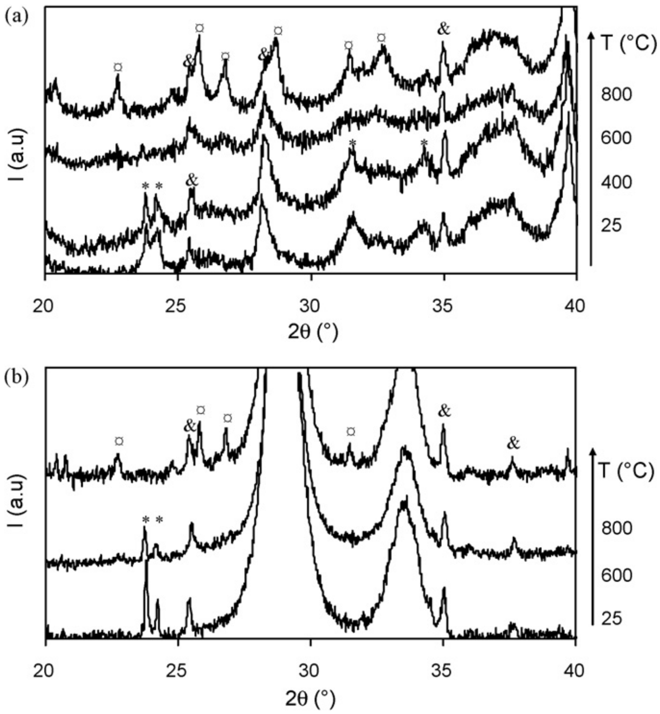

Fig. 5. XRD patterns at 25 °C, 400 °C, 600 °C and 800 °C of sulfated catalysts: (a) Pt/10Ba/Al and (b) Pt/10Ba/CeZr. The catalysts were heated under air from 25 °C up to 800 °C. (¤) $BaSO_4$, (*) $BaCO_3$, (&) support.

after ageing at 600 °C show the appearance of broad peaks corresponding to crystallized $BaSO_4$ (orthorhombic, barite-syn $2\theta = 25.8^\circ$, 26.8°) only for the Pt/10Ba/Al catalyst (Fig. 5a). Finally, further evidence of crystallized $BaSO_4$ was obtained for both catalysts after an annealing treatment at 800 °C. These results indicate that the formation of bulk barium sulfates is retarded on ceria–zirconia compared to alumina.

Otherwise, it can be concluded that ceria–zirconia promotes bulk barium sulfate reduction. Fig. 4c shows that the reduction of these species is completed at 700 °C on Pt/10Ba/CeZr instead of 800 °C on alumina containing samples (Fig. 4a and b). A possible explanation may be given by considering the redox properties of ceria oxide. Indeed ceria can oxidize or reduce molecules depending on the composition of the inlet gas. Ceria (Ce^{4+}) can oxidize a molecule by losing an oxygen atom and a reduced surface (Ce^{3+}) can promote the reduction of a molecule by uptake of an oxygen atom. As the TPR profile of the sulfated Pt/10Ba/CeZr catalyst indicates (Fig. 4c), the reduction of ceria (peak at 250–400 °C) takes place before the reduction of sulfates (peak between 400 and 700 °C). It is then possible that reduced ceria leads to a destabilization of the S–O bonds from the sulfates. Another explanation may be the activation of hydrogen by ceria which will spill-over to the sulfate particles, thus promoting their reduction. For both hypothesis, proximity between ceria and barium is required. Conversely, on the alumina supported catalysts the reduction of large barium sulfates (>10 nm) would not be promoted by hydrogen spill-over [11].

3.5. Regeneration of sulfated and aged catalysts

The TPR profiles of the sulfated and annealed catalysts after regeneration at 550 °C, under a H_2, CO_2 and H_2O containing mixture, are reported in Fig. 6. For comparison, the TPR profiles of sulfated catalysts are also reported. The corresponding hydrogen consumptions and the amounts of remaining sulfur are reported in Table 3. Generally, the

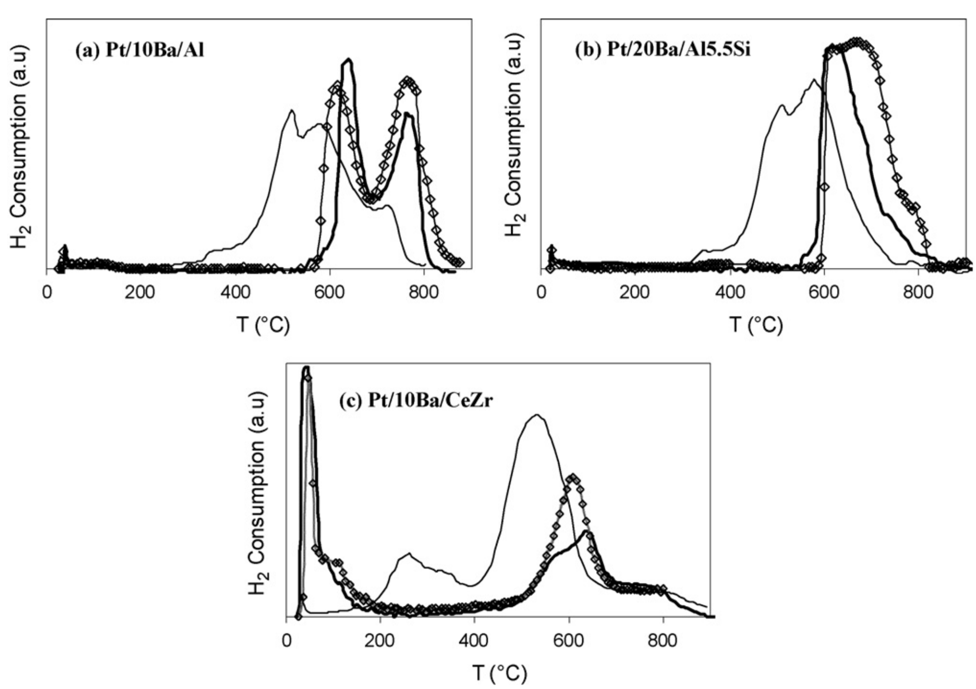

Fig. 6. TPR profiles of (a) Pt/10Ba/Al, (b) Pt/20Ba/Al5.5Si and (c) Pt/10Ba/CeZr. (—) sulfated; (▬) sulfated, aged at 600 °C and then regenerated; (◇) sulfated, aged at 800 °C and then regenerated. The regeneration treatment was carried out at 550 °C under H_2, CO_2, H_2O and N_2 containing mixture.

Table 4
NO_x storage capacities measured at 300 °C on Pt/10Ba/Al, Pt/20Ba/Al5.5Si and Pt/10Ba/CeZr catalysts after different treatments

Catalyst	Treatment							
	Fresh	S	S T600	S T800	S R500	S R550	S T600 R550	S T800 R550
Pt/10Ba/Al	13.8	4.6	7.8	11.1	11.9	15.6	15.3	12.0
Pt/20Ba/Al5.5Si	21.5	11.2	16.6	15.3	18.7	21.0	22.2	15.6
Pt/10Ba/CeZr	12.9	6.4	7.6	8.2	18.2	21.7	24.6	22.4

amount of remaining sulfur increases with the temperature of the ageing treatment before regeneration. This result is in agreement with the formation of stable bulk barium sulfates which is promoted by the rise of the temperature under oxidizing conditions.

The regeneration at 550 °C of sulfated catalysts aged at 600 °C led to a more or less important sulfur elimination depending on catalyst composition: ~15% for the Pt/10Ba/Al catalyst, ~40% for the Pt/20Ba/Al5.5Si and above 60% for the Pt/10Ba/CeZr catalyst. After ageing of the sulfated catalysts at 800 °C, the regeneration treatment is less effective for alumina containing samples with no significant sulfur elimination for the Pt/10Ba/Al catalyst and ~10% for the Pt/20Ba/Al5.5Si. Conversely, more than 50% of sulfur were eliminated for the Pt/10Ba/CeZr sample (Table 4). This result confirms that the ceria–zirconia support plays an important role in barium sulfate elimination under rich conditions.

3.6. NO_x storage capacity of regenerated catalysts

In order to gain information about the efficiency of the regeneration treatment on the different sulfated catalysts, the NO_x storage capacity was measured at 300 °C under a mixture containing 350 ppm NO, 10% CO_2, 10% H_2O and 10% O_2. The results are presented in Table 4. For comparison, the NO_x storages of the fresh (non-sulfated) catalysts are also reported.

The regeneration at 550 °C of sulfated catalysts, led to the total recovery of the initial NO_x storage capacity whatever the catalyst, though some sulfur is still present on the materials, especially for the alumina containing ones. Moreover an increase in NO_x storage capacity is observed after the regeneration treatment for the Pt/10Ba/CeZr catalyst (21.7 μmol g^{-1} after regeneration versus 12.9 μmol g^{-1} for the fresh catalyst). In order to investigate if this increase is linked both to the presence of sulfur and the reducing treatment, the fresh catalyst was treated under the same reducing mixture at 550 °C (H_2, CO_2 and H_2O). The NO_x storage capacity of the fresh catalyst after the reducing treatment increases from 12.9 μmol g^{-1} to 22.8 μmol g^{-1}, indicating that the improvement in the NO_x storage capacity is related only to the reducing treatment. The latter also induces an increase of catalyst oxidation activity (19% versus 7%) which can contribute to the enhancement of the NO_x storage capacity at 300 °C. The same reducing treatment was performed on the Pt/10Ba/Al and Pt/20Ba/Al5.5Si catalysts. The NO_x storage capacities of the fresh catalysts after the reducing treatment at 550 °C were 15.4 and 22.3 μmol g^{-1}, for the Pt/10Ba/Al and Pt/20Ba/Al5.5Si, respectively (13.8 and 21.5 μmol g^{-1} with non-reduced samples). These results show that the promoting effect of the treatment under rich conditions is linked to the presence of the ceria–zirconia oxide [32]. It may result from a migration of cerium from the bulk to the surface during the reducing treatment, as suggested by Fan et al. [28]. The formation of a cerium rich surface could promote the oxidation of NO to NO_2 and the spill over of NO_2 to storage sites.

The decrease of the regeneration temperature of sulfated catalysts to 500 °C led to lower performances whatever the catalyst (Table 4). For the Pt/10Ba/Al, only 85% of the initial NO_x storage properties are recovered, although nearly the same amount of sulfur is eliminated at 500 °C and 550 °C. This result can be explained by the higher migration of sulfates, previously observed for the regeneration treatment at 550 °C (Fig. 3), leading to the recovery of more active Ba surface sites. Likewise, the Pt/20Ba/Al5.5Si catalyst recovered 85% of its initial NO_x storage capacity after regeneration at 500 °C. As for the Pt/10Ba/CeZr catalyst, it shows a lower NO_x storage capacity after regeneration at 500 °C (18.2 μmol g^{-1} versus 21.7 μmol g^{-1} at 550 °C), probably linked to the less effective sulfur elimination previously observed (Table 3).

The annealing treatment at 600 °C of sulfated catalysts did not modify the efficiency of the regeneration at 550 °C. Indeed, sulfated catalysts annealed at 600 °C and sulfated catalysts show the same performances after regeneration at 550 °C (Table 4). On the other hand, the regeneration treatment leads to lower NO_x storage trapping properties on sulfated Pt/10Ba/Al and Pt/20Ba/Al5.5Si catalysts annealed at 800 °C, while the Pt/10Ba/CeZr catalyst presents similar NO_x storage capacities, whatever the ageing temperature. The different behaviors observed on alumina containing catalysts compared to the ceria–zirconia one can be explained by a higher sintering of the Ba component on the formers. Indeed, the TPR of sulfated catalysts previously reported in Fig. 4, have shown that the amount of bulk barium sulfates was strongly enhanced after ageing at 800 °C. In order to check this hypothesis, the fresh Pt/10Ba/Al and Pt/20Ba/Al5.5Si catalysts were annealed at 800 °C and then treated in rich conditions at 550 °C before NO_x storage measurements at 300 °C. The values obtained were close to that reported in Table 4 for the sulfated samples annealed at 800 °C and regenerated at 550 °C (S T800 R550): 12.3 μmol g^{-1} versus 12.0 μmol g^{-1} for Pt/10Ba/Al and 15.4 μmol g^{-1} versus 15.6 μmol g^{-1} for Pt/20Ba/Al5.5Si.

4. Conclusion

The influence of the support oxide (Al_2O_3, Al_2O_3–5.5 wt%SiO_2 and $Ce_{0.7}Zr_{0.3}O_2$) as well as the Ba loading

was studied with regard to sulfur resistance and regeneration. Barium sulfate stability was influenced by the support oxide and the Ba loading. For alumina containing catalysts the amount of deposited sulfur and sulfate stability under hydrogen increase with the Ba loading. Conversely, no modification in barium sulfates stability was observed for Ce–Zr supported samples, whatever the Ba loading. Furthermore, for the latter support, a decrease of the amount of deposited sulfur with the increase of Ba loading was noticed. This result was explained by both a decrease of the BET surface area and the limitation of SO_x diffusion due to higher barium crystallite size.

Ageing at 600 °C under oxidizing conditions of the sulfated Pt/10Ba/Al catalyst led to the formation of crystallized $BaSO_4$ detected by XRD. Their presence was observed only after ageing at 800 °C under the same conditions for Pt/10Ba/CeZr. Moreover, ceria–zirconia led to a decrease of bulk $BaSO_4$ stability under hydrogen, their reduction temperature being about 100 °C lower than on alumina containing materials. The sulfates elimination under rich conditions (H_2, CO_2, H_2O, N_2) was more efficient on ceria–zirconia supported sample: 85–90% of sulfur are eliminated at 550 °C on Pt/10Ba/CeZr while only 55% and 40% are eliminated on Pt/10Ba/Al and Pt/20Ba/Al5.5Si, respectively. The same trend was observed on sulfated catalysts annealed at high temperature (600 °C and 800 °C) before regeneration, but to a less extent.

Sulfation of the catalysts induced a loss of the NO_x storage capacity (measured in the presence of 10% CO_2 and 10% H_2O) that ranges between 50% and 70%, depending on catalyst composition. All the catalysts recovered their initial NO_x storage capacity after regeneration at 550 °C, even with an improvement in the case of CeZr containing material. This behavior is linked mainly to the reduction of ceria during the rich treatment. Eventually, the ageing at 800 °C of sulfated catalysts before regeneration did not lower significantly the performance of the Pt/10Ba/CeZr catalyst, contrary to the alumina containing samples.

In conclusion, concerning sulfur deactivation of NO_x storage catalysts, the results reported in the present work show the interest to include ceria–zirconia in the composition of NSR catalysts.

Acknowledgments

This work was financially supported by the French Environment and Energy Management Agency (ADEME) and the Poitou-Charentes Region.

References

[1] N. Miyoshi, S. Matsumoto, K. Katoh, J. Harada, N. Takahashi, K. Yokota, M. Sugiura, K. Kasahara, SAE Tech. Paper 950809, 1995.
[2] W.S. Epling, L.E. Campbell, A. Yezeerets, N.W. Currier, J.E. Parks II., Catal. Rev. 46 (2004) 163.
[3] H. Mahzoul, L. Limousy, J. Brilhac, P. Gilot, J. Anal. Appl. Pyrol. 56 (2000) 179.
[4] S. Matsumoto, Y. Ikeda, H. Suzuki, M. Ogai, N. Myoshi, Appl. Catal. B 25 (2000) 115.
[5] S. Elbouazzaoui, E.C. Corbos, X. Courtois, P. Marecot, D. Duprez, Appl. Catal. B 61 (2005) 236.
[6] H. Abdulhamid, E. Fridell, J. Dawody, M. Skoglundh, J. Catal. 241 (2006) 200.
[7] C. Sedlmair, K. Seshan, A. Jentys, J. Lercher, Catal. Today 75 (2002) 413.
[8] F. Rohr, U. Gobel, P. Kattwinkeller, S. Philipp, P. Gélin, Appl. Catal. B 70 (2007) 189.
[9] C. Courson, A. Khalfi, H. Mahzoul, S. Hodjati, N. Moral, A. Kiennemann, P. Gilot, Catal. Comm. 3 (2002) 471.
[10] S. Poulston, R.R. Rajaram, Catal. Today 81 (2003) 603.
[11] X. Wei, X. Liu, M. Deeba, Appl. Catal. B 58 (2005) 41.
[12] Z. Liu, J. Anderson, J. Catal. 228 (2004) 243.
[13] H. Mahzoul, P. Gilot, J.F. Brilhac, B.R. Stanmore, Top. Catal. 16–17 (2001) 293.
[14] J. Dawody, M. Skoglundh, L. Olsson, E. Fridel, Appl. Catal. B 70 (2007) 179.
[15] Ch. Sedlmair, K. Seshan, A. Jentys, J.A. Lercher, Catal. Today 75 (2002) 413.
[16] A. Amberntsson, M. Skoglundh, S. Ljungstrom, E. Fridell, J. Catal. 217 (2003) 253.
[17] K. Yamazaki, T. Suzuki, N. Takahasi, K. Yojota, M. Sugiura, Appl. Catal. B 30 (2001) 459.
[18] F. Basile, G. Fornasari, A. Grimandi, M. Livi, A. Vaccari, Appl. Catal. B 69 (2006) 58.
[19] J. Xiao, X. Li, S. Deng, F. Wang, L. Wang, Catal. Comm. 8 (2007) 926.
[20] S. Hodjati, C. Petit, V. Pitchon, A. Kiennemann, Appl. Catal. B 30 (2001) 247.
[21] H.Y. Huang, R.Q. Long, R.T. Yang, Appl. Catal. B 33 (2001) 127.
[22] N. Takahashi, A. Suda, I. Hachisuka, M. Sugiura, H. Sobukawa, H. Shinjoh, Appl. Catal. B 72 (2007) 187.
[23] K. Yamamoto, R. Kikuchi, T. Takeguchi, K. Eguchi, J. Catal. 238 (2006) 449.
[24] G. Centi, G. Fornasari, C. Gobbi, M. Livi, F. Trifirò, A. Vaccari, Catal. Today 73 (2002) 287.
[25] J.M. Clacens, R. Montiel, H. Kochkar, F. Figueras, M. Guyon, J.C. Beziat, Appl. Catal. B 53 (2004) 21.
[26] E.C. Corbos, X. Courtois, N. Bion, P. Marecot, D. Duprez, Apll. Catal. B 76 (2007) 357.
[27] J. Dawody, M. Skoglundh, L. Olsson, E. Fridell, J. Catal. 234 (2005) 206.
[28] J. Fan, X. Wu, R. Ran, D. Weng, Appl. Surf. Sci. 245 (2005) 162.
[29] M.F. Luo, X.M. Zheng, Appl. Catal. A 189 (1999) 15.
[30] M. Waqif, P. Bazin, O. Saur, J.C. Lavalley, G. Blanchard, O. Touret, Appl. Catal. B 11 (1997) 193.
[31] P. Engström, A. Amberntsson, M. Skoglundh, E. Fridell, G. Smedler, Appl. Catal. B 22 (1999) L241.
[32] F. Fally, V. Perrichon, H. Vidal, J. Kaspar, G. Blanco, J.M. Pintado, S. Bernal, G. Colon, M. Daturi, J.C. Lavalley, Catal. Today 59 (2000) 373.